Chapter 11
Generalized Design Methodology for Three-Arm Spiral Cut Compliant Linear Stage

Kiran Bhole and Sachin Mastud

Abstract This paper presents generalized design methodology of compliant mechanism-based linear stage consisting of three-arm spiral cut flexible linkages. Determination of geometrical parameters of spiral cut and other attributes of compliant mechanisms for required displacement is being major focus of the study. Hence, the study presents systematic investigation of effect of parameters of compliant mechanisms on displacement of stage as an outcome. This parametric study is conducted using finite element platform ANSYS. Various parameters considered in the study are spiral angle, thickness of the flexural plate, and width of spiral cut. These factors are varied at different levels to observe its effect on stiffness of the compliant mechanisms responsible for displacement of the linear stage. The findings of the simulation study are represented in dimensionless terms for its generalization and further validated through sample experiential study. Based on non-dimensional analysis, design chart is prepared for determination of geometrical parameters of similar class of compliant mechanisms.

Nomenclature

d	Outer diameter of flexural disc, mm.
l	Distance between stacks of flexural discs, mm.
m	Distance between consecutive flexural discs in a stack, mm.
n	Number of spiral arm.
t	Thickness of flexural spiral disc, mm.
w	Width of the spiral arm, mm.

K. Bhole (✉)
Department of Mechanical Engineering, Sardar Patel College of Engineering Andheri, 400058 Mumbai, India
e-mail: kiran_bhole@spce.ac.in

S. Mastud
Department of Industrial and Production Engineering, Veermata Jijabai Technological Institute, 400019 Matunga, Mumbai, India

A. Sachdeva et al. (eds.), *Operations Management and Systems Engineering*,
Lecture Notes on Multidisciplinary Industrial Engineering,
https://doi.org/10.1007/978-981-15-6017-0_11

θ Spiral turn angle, degrees.
E Young's modulus of elasticity, N/m^2.
F Actuating force in z-direction, N.
P Pitch of the spiral arm, mm.
S Spiral cut width, mm.
Z Axial displacement of flexural system in z-direction under actuating force, mm.
K_a Axial stiffness, N/mm.
K_r Radial stiffness, N/mm.

11.1 Introduction

High accuracy and precision are the prominent features of compliant mechanisms. These features are attained due to bending of flexible elements of the mechanisms. Hence, these mechanisms are used in transmitting force and motion without any loss [1–6]. Joint-free linkages and no friction make mechanism highly accurate in transmitting motion. The absence of stiction and backlash are also important characteristics of these mechanisms. Further, these characteristics lead to maintenance and lubrication-free mechanisms. Here, it is to be noted that the flexible linkages are set to deform well below elastic limit for its successful execution. Hence, compliant mechanism is useful for low range of force and motion transmissions. Typically, flexures are used in micro-electromechanical systems, linear stages in micro-manufacturing [7–10], robotics, cryogenic applications [11, 12], and so on. Different designs of flexural systems are used by researchers to achieve different high-end requirements in sophisticated applications. Double parallelogram types of flexural systems are used for steering the laser beam in the opto-mechatronic system for on-axis micro-stereo lithography [8, 13–15] and compact disc of computing devices. Zero parasitic error due to compliant deformation of flexural beams enables flexures to allow exact linear steering of laser beam with nanometre resolution. Monolithic flexural mechanisms are also developed for guiding the cutting tool or workpiece in high precision micro-drilling and turning centres [3, 7, 9, 10]. Mechanism consisting of a parallel flexure hinge is utilized in ultra-precision turning operation to guide the moving platform and to preload the piezoelectric actuator. The developed mechanism has shown resolution up to 12 nm with reduced hysteresis and linearity of output. Furthermore, researchers have reported state-of-the-art design of the flexural mechanisms for nano-positioning of high-speed scanning probe used in video rate atomic force microscopy and probe-based nanofabrication.

Various geometrical variants of flexible elements are used in compliant mechanisms [2, 16–19]. Circular disc with spiral shape cuts through it is one of the variants of flexible elements [11, 20–22]. This spiral cut flexible element makes member low stiffness, thus making element easy to bend in axial direction under the application of axial force. Although axial stiffness is low, member intact its high radial stiffness [11]. These spiral cut flexural elements were used initially for measurement of

earth vibrations due to its inherent high sensitivity. Further due to high accuracy in linear guidance with no requirements of lubrication, these are used in Stirling engine for cryogenic applications. Towards analysis of these flexible elements, study has presented parametric synthesis of single-disc spiral slot flexural linear stage through dynamic and modal loads [23]. Identification of best geometrical parameters for maximum life of linear stage and highest possible ratio of radial to axial stiffness were central theme of the study. Based on synthesis, the study has presented graphical data sheet to select best possible configuration of the flexural disc for the given input parameters. However, study also recommends the finite element (FE) analysis to tune the parameters. Spiral-shaped flexural elements with multiple discs in a stack and with such multiple stacks in assembly are used in applications for accurate linear movement with robustness. Design guidelines for such spiral cut flexural linear stage consisting of multistacked discs are not yet presented in generalized way. Hence, this paper presents the generalized design methodology for the multidisc, multistage, three-arm spiral cut compliant mechanism. Design methodology is based on simulation and experimental study conducted on compliant mechanism. In derived design methodology, outer and inner diameters and thickness of the three-arm spiral cut discs are considered as input conditions. Geometrical parameters of the disc, viz spiral turn angle, width of spiral cut, and pitch of the spiral, are the typical outputs of the design procedure for the required linear displacement.

11.2 Configuration of Spiral Slot Flexural Stage

It is important to understand geometrical attributes and nomenclature of the spiral cut circular flexural disc used in the study. Figure 11.1 shows the flexural disc considered

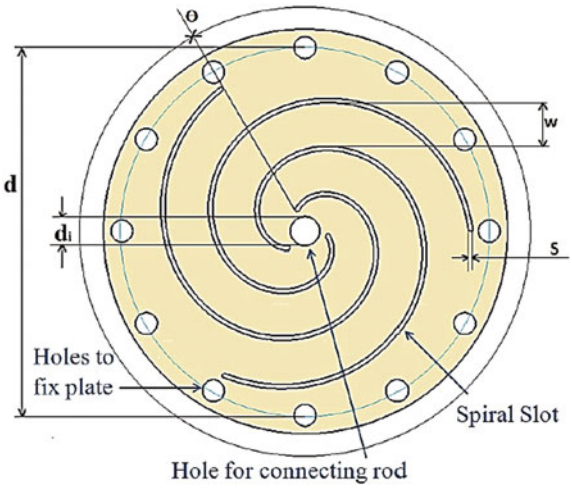

Fig. 11.1 Drawing of the spiral cut flexure disc for compliant linear stage

in this study. The spiral cut on the disc is normally done through wire cut electrodischarge machining process. Here, it is to be noted that the number of spiral-shaped cuts on the circular disc are referred as number of spiral arms. Further, the angle between start and end points of spiral cut is defined as spiral turn angle. Illustrated flexural disc in Fig. 11.1 demonstrates three-arm flexural discs with geometrical notations as defined in nomenclature. The assembly of these discs to form linear stage is demonstrated in Fig. 11.2. Assembly consists of two stacks of flexural disc (refer Fig. 11.2). Each stack of the flexural disc consists of two discs. These two flexural stacks are separated by intermediate spacers at the inner and outer periphery of the disc. Further, the formed stack of the flexural disc is connected with other stack with the help of rigid connector at the centre. The flexural discs are held fixed at the outer periphery, but free to bend along the central axis under the actuating force in *z*-direction. Specifically, this paper presents first the analysis of this form of the flexural assembly. In analysis, the linear displacement of the flexural assembly is measured against the actuating force, F. Desired linear displacement of the flexural assembly in the direction of actuating force (z direction) is of interest in the study. Various parameters of flexural disc and assembly considered in the study are presented in Table 11.1. These parameters are considered based on literature study [11]. Generally, stainless steel or copper beryllium (copper alloy with 0.5–3% beryllium) material is found most suitable due to their flexural properties in compliant mechanism. Copper beryllium is most preferred material in compliant mechanism due to ability of stress relaxing during bending [24]. Hence, copper beryllium material is considered in the study (refer Table 11.1 for properties of copper beryllium).

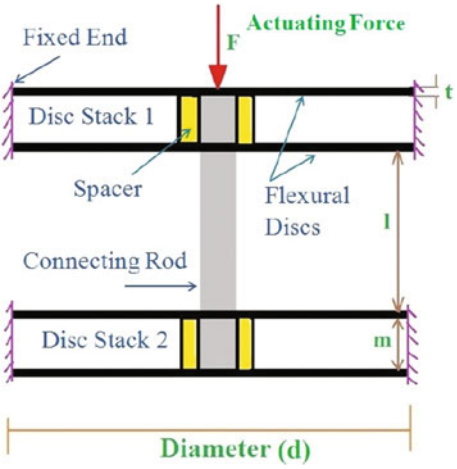

Fig. 11.2 Schematic of stack of flexure disc forming flexural linear stage

Table 11.1 List of parameters of system and material properties of flexural disc

Parameters	Value
Spiral arms	3
Number of flexural stacks	2
Number of flexural discs in stack	2
Distance between consecutive stacks	50 mm
Distance between consecutive discs	3 mm
Young's modulus of Copper Beryllium	165 x 10^9 N/m^2
Density of Copper Beryllium	8150 kg/m^3
Poisson's ratio of Copper Beryllium	0.3

11.3 Characterization of Spiral Arm Flexural Stage

Figure 11.3 shows the CAD model of flexural system prepared according to specifications (refer Table 11.1) in the modelling software CATIA. The prepared model is then imported in FE platform ANSYS for the purpose of characterization. The model consists of two-stage three spiral arm flexural linear stage. Dimensions of geometric attributes mentioned in Fig. 11.1 of the flexural bearing are shown in Table 11.1. The relation between arm width and slot thickness is given by derived parameter, pitch, by Simon Amoedo et al. [24]. Pitch changes with change in slot width for constant outer diameter and spiral angle. Equation (1) presents relation for pitch in terms of

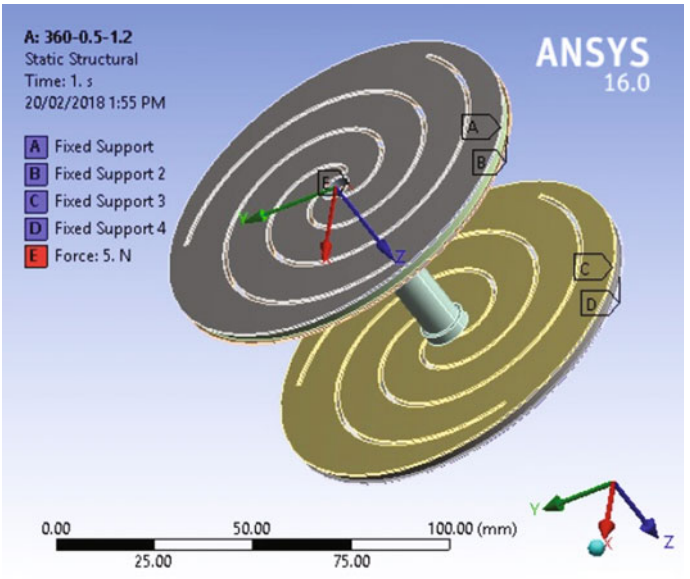

Fig. 11.3 Model of three-arm double discs and stacks flexural linear stage with boundary conditions

arm width, width of slot, and number of spiral arms [24].

$$P = w(n - s) \tag{1}$$

The flexural linear stage is characterized for its axial displacement and developed axial and radial stiffness for the actuation force using FE platform, ANSYS. The actuation force of 5 N is considered for the characterization. Study [24] has revealed factors, viz thickness of disc, slot width of spiral slot, and spiral turn angle being most important for controlling stiffness of the compliant mechanism. Design of experiments is conducted on the selected flexural linear stage. Table 2 shows the factors and their levels for the designed experiments. Four levels (L) of each of the three factors (F) are considered in the study (refer Table 2). To reveal accurate influence of parameters, full factorial design is proposed in the study. Hence, LF = 64, number of experiments were performed in finite element platform, ANSYS. In the analysis, boundary conditions prescribed on the linear stage as (1) rim of circular disc being fixed (refer Fig. 11.1), (2) central portion is free to move (in the direction of actuating force). The actuating force is applied on the central portion of the compliant linear stage in z-direction. Due to prescribed boundary conditions, the flexural elements (spiral cuts discs) bends (refer Fig. 11.4 resulting significant linear displacement in the direction of applied force. Before applying complete proposed design of experiments, the trial experiments are conducted on two stacks with two discs in stack assembly of compliant linear test stage. The spiral cut on the discs is having turn angle of 360° with width of cut being 1.2 mm. Further, plate thickness

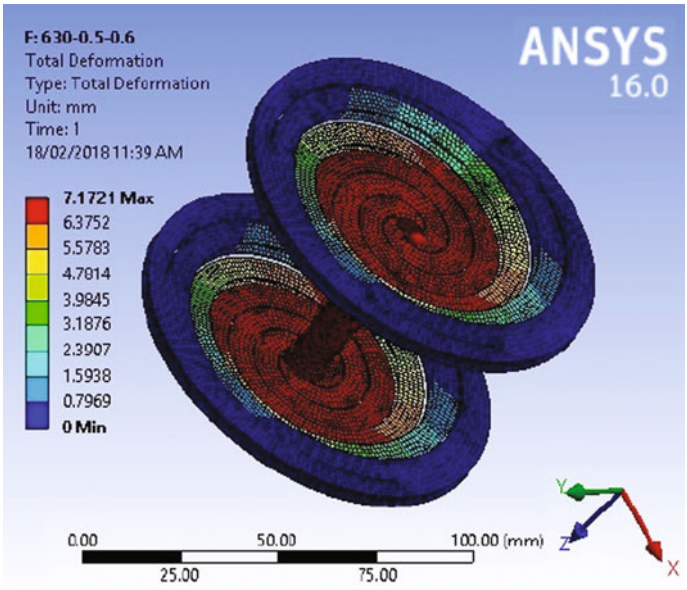

Fig. 11.4 Fe analysis for displacement of three-arm double discs and stacks flexural linear stage

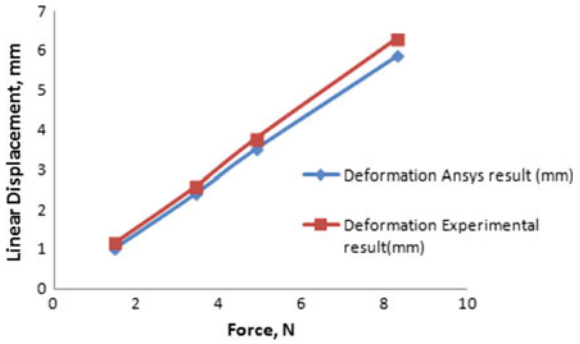

Fig. 11.5 Comparison of simulation and experimental results for validity

in fabricated compliant test stage is of 0.25 mm. The central static load is varied on the fabricated test stage from 2 to 10 N. Central displacement due to these static forces is measured with the help of linear encoder (Renishaw). The characteristics of this experimental test stage are shown in Fig. 11.5 along with the simulation results conducted on similar test model in ANSYS. Figure 11.5 shows good agreement between the simulation and experimental results. Henceforth, the simulations are conducted on different cases of compliant stage according to design of experiments.

Stiffness is one of the important characteristics in design of compliant system. The amount of linear movement of the compliant stage is dependent on its stiffness. Lower stiffness in the direction of desired direction of motion is desirable, while higher stiffness is required in the other mutually perpendicular directions. Hence, typically for the stage under study, low axial (z-direction) stiffness and high radial stiffness are required. Thus, in the characterization of this stage, central displacement (z-direction) and radial displacement under application of axial force are obtained through simulations. The axial actuating force is kept constant in all the simulations, while factors are varied at various levels (refer Table 2) for the wide range of simulation. From obtained axial and radial deformations, the axial and radial stiffness are determined. For generalization of the characteristics, the obtained displacement and stiffness are normalized. The outer diameter of the disc, thickness of the disc, total number of discs in the stack, number of discs in the stacks, and characteristics of spiral cut (profile of spiral, width of spiral cut, spiral turn angle, number of arms of spiral) are the parameters governing stiffness of the compliant stage. Overall among these various factors, it is very important to find factors having most influence on stiffness. For generalization of results, factors of the complaint stage are normalized by dividing them with outer diameter of the disc. Thus, axial displacement, slot width, thickness, and pitch are presented in dimensionless forms as z/d, s/d, t/d, and p/d, respectively. Further, axial and radial stiffness of the flexural bearing is presented in dimensionless form as $\frac{K_a \times 10^{-8}}{E \times d}$ and $\frac{K_r \times 10^{-8}}{E \times d}$, respectively. Inline with these normalized parameters, influence of factors on stiffness is presented in the following subsections.

11.3.1 Effect of Slot Width on Stiffness

Figure 11.4 shows one of the results for displacement of flexural system under the application of force 5 N in z-direction. Figure 11.4 depicts the zero displacement at the periphery of the disc due to applied boundary condition of fixed outer rim and maximum displacement at the central portion due to bending of spiral elements. For the characterization, maximum deformation at the central portion of the stage is recorded and presented as dimensionless displacement. Based on the maximum deformation, dimensionless axial and radial stiffness are evaluated. Figure 11.6 shows the effect of normalized slot width on the axial and radial stiffness of the flexural system of two stacks for cases consisting of two and three discs (layers) in a stack. In both the cases, 0.5 mm disc thickness and spiral angle 630° are considered. Figure 11.6 reveals decrease in axial and radial stiffness with increase in dimensionless slot width. This observation is similar in compliant stage consisting of double and triple flexural discs in a stack. This implies that complaint stage will provide more deformation with increase in slot width for constant actuating force. This is because increase in slot width decreases the rigidity of the system and increase in flexibility. Further, it is noted that the deformation in double-layer flexural system is more compared to the three layers flexural system as later is less flexible. This leads to high stiffness in triple-layer system compared to double-layer flexural system (see Fig. 11.6). Further, characterization shows that the change in axial stiffness is less as compared to the change in radial stiffness (refer Fig. 11.6). Hence, the slot width effect is more dominantly seen on the radial stiffness of spiral-based flexural system. From design aspects for the linear motion of the flexural system, the axial deformation of the system is most desired, while radial deformation of the system is not favourable. Hence, from this consideration, appropriate selection of spiral slot width shall be done based on obtained characteristics. Further to present design guidelines for deciding the spiral slot width and thickness of disc, characteristics presented in Fig. 11.6 are presented in terms of stiffness ratio (refer Fig. 11.7). This characteristic can be used to decide the spiral slot width based on selected axial and radial stiffness and normalized thickness of the flexural disc.

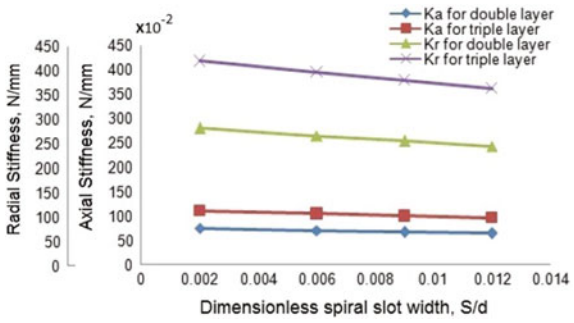

Fig. 11.6 Radial and axial stiffness against dimensionless spiral slot width

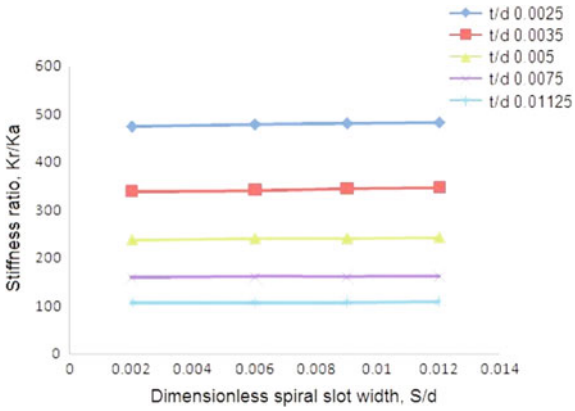

Fig. 11.7 Stiffness ratio against dimensionless spiral slot width

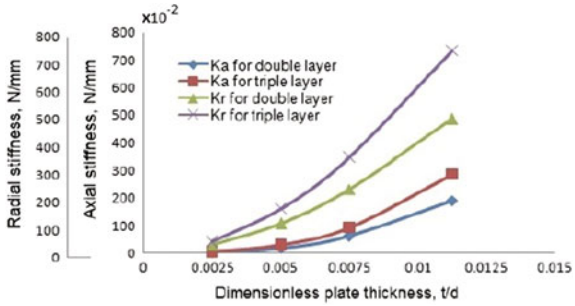

Fig. 11.8 Radial and axial stiffness against dimensionless thickness

11.3.2 Effect of Disc Thickness on Stiffness

Figure 11.8 shows the effect of thickness of disc on axial and radial stiffness. The stiffness characteristics are presented for constant dimensionless slot width of 0.006 (slot width of 0.6 mm for the case presented) and spiral angle of 1080° against dimensionless thickness. The characteristics show large change in both axial and radial stiffness (refer Fig. 11.8) beyond normalized thickness 0.0075. These characteristics are observed in case of both two- and three-layer flexural system. However, magnitude of stiffness of the three layers system is more compared to two layers as addition of layer contributes towards more rigidity of the system opposing flexibility or deformation.

11.3.3 Effect of Spiral Turn Angle on Stiffness

Figure 11.9 shows the effect of spiral turn angle on axial and radial stiffness of the compliant linear system. Characteristics (refer Fig. 11.9) depict decrease in axial

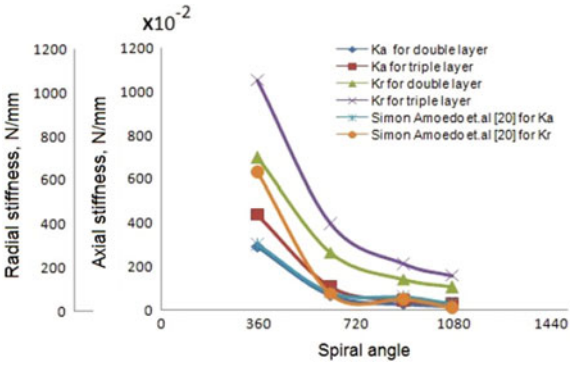

Fig. 11.9 Radial and axial stiffness against spiral turn angle

stiffness allowing more deflection with increase in spiral turn angle. This observation in characteristics is seen for both double- and triple-layer compliant linear system. Increase in spiral angle in constant diameter disc leads to decrease in arm width. This decrease in arm width leads to decrease in axial stiffness allowing more deformation of the system. The obtained characteristics are compared with the similar characteristics obtained by Simon Amoedo et al. [24]. Figure 11.9 also shows the decrease in radial stiffness with increase in spiral angle for the similar set of flexural system. Similar effect of decrease in arm width is responsible for attenuation in radial stiffness. The nature of characteristics for double and triple layers of discs in a stack is also similar to that in study presented by Simon et al. [24] for single-disc flexural element.

11.4 Discussion

Based on the analysis, following are the summary points from the designed experiments for characterization on the stiffness of the compliant linear stage:

1. Increase in slot width of spiral cut decreases both axial and radial stiffness.
2. Increase in thickness of spiral flexural disc increases both axial and radial stiffness.
3. Increase in spiral turn angle decreases both axial and radial stiffness.

It is logical that increase in thickness of flexural discs, number of stacks, and number of flexural discs increase rigidity of the stage and hence increase the stiffness of the disc. On other hand, increase in outer diameter of disc makes disc to deform more under bending, thus causing decrease in stiffness. Furthermore, similarly increase in characteristics of spiral cut (width of spiral cut, spiral turn angle, number of arms of spiral) makes discs more hollow resulting in decrease in stiffness.

For the purpose of generalization towards generating the design methodology for similar flexural system, the results of characterization are required to be presented in the form of ratio of dimensionless stiffness. Further, the axial displacement is one

of the important requirements to be fulfilled while designing flexural system used as linear guide ways or scanning mechanisms. Considering these specific requirements, the characteristics are presented in terms of dimensionless displacement and dimensionless stiffness. Figure 11.10 shows the characteristics of the flexural system representing dimensionless axial stiffness against dimensionless displacement (feed), and Fig. 11.11 shows the dimensionless radial stiffness against dimensionless displacement for various dimensionless thicknesses. Figure 11.10 shows lesser variation in dimensionless axial stiffness against dimensionless displacement for lower dimensionless thickness (refer characteristics for dimensionless thickness 0.0054 and 0.0038 in Fig. 11.10). Further, it is observed that stiffness tends to saturate beyond dimensionless displacement of 0.08. However, the significant dependency of dimensionless axial stiffness on dimensionless thicknesses is noted from the characteristics. Figure 11.11 depicts that significant variation in dimensionless radial

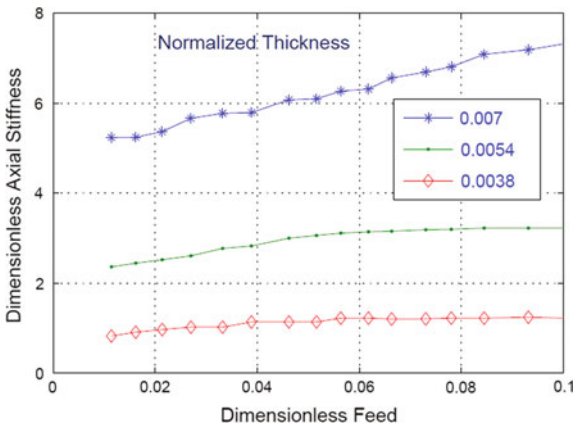

Fig. 11.10 Dimensionless axial stiffness against dimensionless displacement of the flexural linear stage

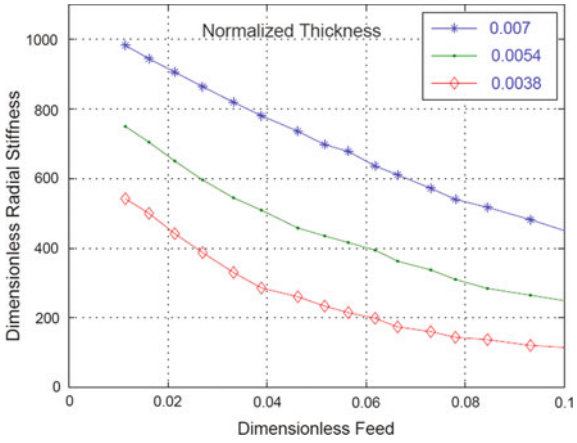

Fig. 11.11 Dimensionless radial stiffness against dimensionless displacement of the flexural linear stage

stiffness against dimensionless axial displacement. High dimensionless radial stiffness is observed at lower dimensionless axial displacement. Further, it is observed that dimensionless radial stiffness increases with increase in dimensionless thickness. Low axial stiffness provides good sensitivity for displacement in feed direction, while high radial stiffness signifies high resistance to deformation in lateral direction against applied force. Hence, characterization points that flexural stage gives better linear guidance for dimensionless feed within 0.08. Hence, the regime up to dimensionless feed 0.08 is recommended for the spiral type of flexural stages. Figures 11.10 and 11.11 depict consolidated view of the stiffness and geometrical parameters of the flexural system. Hence, this characteristic can be taken as one of the references for generating design guidelines for the flexural system.

11.5 Graphical Design Chart

Figure 11.12 shows the design chart for the three-arm, two-stack spiral-shaped flexural system based on the characterization presented in above sections. The methodology of graphical design tool presented is similar to the design methodology reported first time for single-disc flexural system by Simon Amoedo et al. [24]. This tool is developed to minimize the time required for optimizing the specific flexural system for application which requires large number of FE simulations. Set of parameters in this developed design tool are in dimensionless term to have generalization. For use of design chart, it is necessary to choose the basic input parameters of the flexural systems along with the desired requirement from the system based on the intended application. For the use of developed design chart, designer is expected to start with input parameters. Here, the designers input parameters are outer diameter and inner diameter of flexural system, material properties, and desired axial displacement "z". The designers seek parameters of flexural system, viz thickness of flexural disc, slot width, and spiral angle from the graphical design chart. The step-by-step procedure depicting use of developed design chart is presented in next section.

11.6 Design Procedure

To start with design, initially the designer has to decide final output desired from the stacked flexure assembly and predetermined diameters of the flexural discs for intended application. Typical of desired output for flexural system used for linear guide ways is axial displacement under applied actuating force. The desired axial displacement is generally needed with ideally zero radial displacement and stress in the flexural element below limiting level. This is taken into consideration in the development of design chart derived based on FE simulations discussed in the previous section. For the user, the design procedure to be adopted is summarized as below:

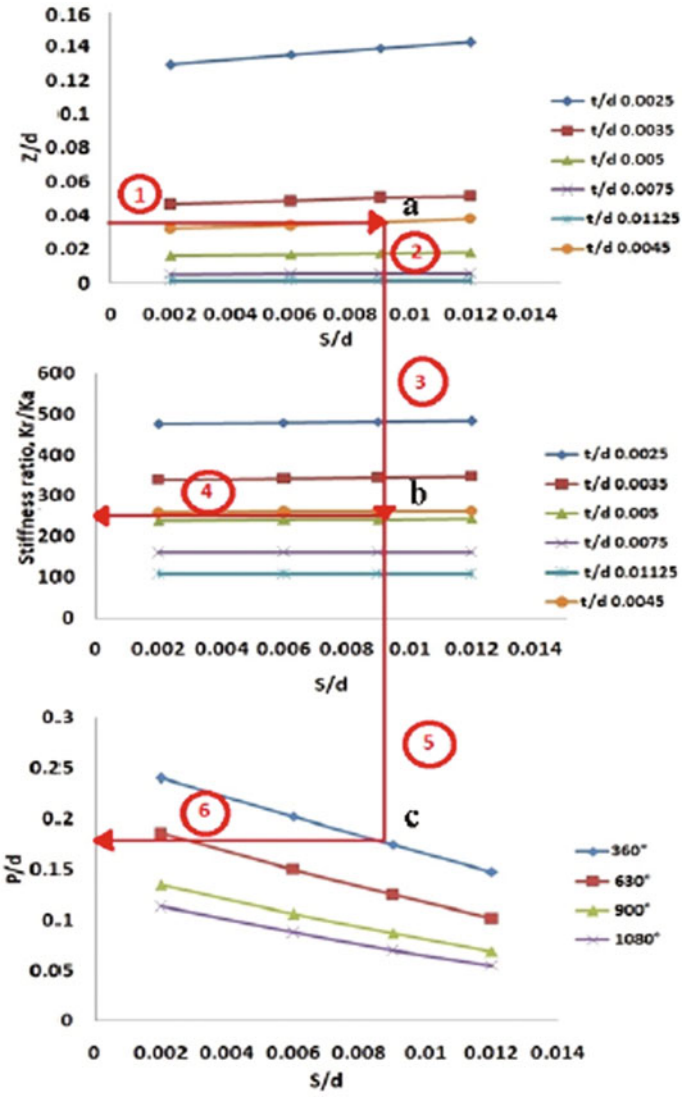

Fig. 11.12 Design chart and process methodology for two-stack three-arm flexure linear stage

1. Determine outer diameter, d of the flexural disc as design input.
2. Determine maximum axial displacement, Z as required for the application for which linear stage is to be designed.
3. Derive dimensionless axial displacement (Z/d) required as primary input to use design chart.
4. Draw horizontal line from dimensionless axial displacement obtained from step 3 (refer horizontal line 1 in graph Z/d versus S/d in Fig. 11.12).

5. Obtain point of intersection of constant dimensionless displacement line with lines of constant dimensionless thickness (t/d) (refer point "a" Fig. 11.12).
6. Calculate thickness of the flexural disc (t) from the dimensionless thickness obtained from Step 5.
7. Draw vertical line from point of intersection "a" on x-axis to obtain dimensionless spiral slot width, S/d
8. Calculate slot width of spiral from obtained dimensionless slot width of spiral.
9. Draw vertical line (refer vertical line 2 in Fig. 11.12) from point of intersection "a" to obtain point "b" on line of selected dimensionless thickness in graph of K_r/K_a versus S/d in Fig. 11.12.
10. Obtain K_r/K_a from point of intersection "b". Review the ratio K_r/K_a of the system (refer horizontal line 4 in Fig. 11.12). Low K_r/K_a ratio is desirable for the flexural system used for accurate linear positioning application with better sensitivity for displacement in axial direction. Designer may seek alternatives to get optimum K_r/K_a considering accuracy and sensitivity. If designer seek alternatives shall iterate steps 1–10 for best fit in design.
11. Draw vertical line from point "b" (refer vertical line 5 in Fig. 11.12) on graph P/d versus S/d to get point of interaction "c" for desirable spiral turn angle. Here, various options for spiral turn angle are available for the designer.
12. From point "c", dimensionless pitch can be obtained from graph P/d versus S/d (refer horizontal line 6 in Fig. 11.12). From obtained P/d, pitch can be calculated. Calculated pitch can be used to determine width of spiral arm from Eq. (1). Width of the spiral arm will be dependent on the spiral turn angle selected. Consideration of design for manufacturing may be applied to select the spiral turn angle and thus arm width.

From application of above steps, it is possible to design three-arm two stacks with each stack of two-disc spiral-shaped flexural system. Based on the developed design methodology, compliant linear feed stage is designed. Figure 11.13 shows the developed compliant linear feed stage for micro-drilling workstation. In the design of the feed stage, the linear displacement of 6.5 mm is considered for the two-disc two-stack compliant linear stage. Further, outer diameter of flexural disc is considered to be 110 mm. With these input data, the developed methodology is applied to obtain various parameters of spiral cuts. On application of the derived data in developed linear complaint stage, the desired linear displacement is obtained for the micro-drilling.

11.7 Conclusions

FE analysis is carried on different combination of parameters for spiral flexure assembly consisting of three arm and two stacks (each stack consists of two discs). Effect of these parameters on radial and axial stiffness is studied, and the results are plotted in the form of charts for simple understanding. Further, the effect of these

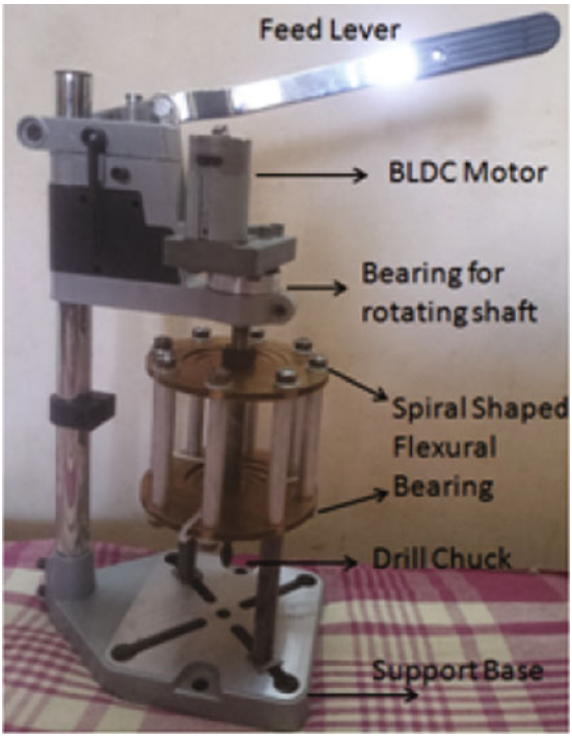

Fig. 11.13 Photograph of developed compliant linear feed stage for micro-drilling

parameters on axial displacement is also studied. Based on this characterization, a design procedure is developed for system designer. Developed design chart enables designer to choose optimum geometrical dimensions of flexural discs in flexure assembly for desired outcome (typically the axial displacement of flexural system). The design procedure is recommended for constant distance between plates, three-arm spiral and two-stack system. Effect of these parameters can be studied further to seek more alternatives in design.

Acknowledgements Authors would like to acknowledge financial support for this work by Science and Engineering Research Board (SERB) of Government of India (Project reference number ECR/2016/000760). Authors also acknowledge the support of Sardar Patel College of Engineering, Andheri, Mumbai, to carry out the project work.

References

1. Stephen, A., Schrauf, G., Mehrafsun, S., Vollertsen, F.: High speed laser micro drilling for aerospace applications. Procedia CIRP **24**, 130–133 (2014)
2. Gandhi, P., Deshmukh, S.: A 2D optomechanical focused laser spot scanner: Analysis and experimental results for microstereolithography. J. Micromech. Microeng. **20**, 015035 (2009)

3. Tian, Y., Zhang, D., Shirinzadeh, B.: Dynamic modelling of a flexure-based mechanism for ultra-precision grinding operation. Precis. Eng. **35**, 554–565 (2011)
4. Guo, Z., Tian, Y., Liu, C., Wang, F., Liu, X., Shirinzadeh, B., Zhang, D.: Design and control methodology of a 3-DOF flexure-based mechanism for micro/nano-positioning. Robot. Comput.-Integr. Manuf. **32**, 93–105 (2015)
5. Wang, R., Zhou, X., Zhu, Z.: Development of a novel sort of exponent-sine-shaped flexure hinges. Rev. Sci. Instrum. **84**, 095008 (2013)
6. Tian, Y., Shirinzadeh, B., Zhang, D.: A flexure-based mechanism and control methodology for ultra-precision turning operation. Precis. Eng. **33**, 160–166 (2009)
7. Luo, H., Zhang, B., Zhou, Z.: A rotary flexural bearing for micromanufacturing. CIRP Ann. **57**, 179–182 (2008)
8. Gandhi, P., Bhole, K.: Characterization of "Bulk Lithography" process for fabrication of three-dimensional microstructures. J. Micro Nano-Manufacturing **1**, 041002 (2013)
9. Tian, Y., Shirinzadeh, B., Zhang, D.: A flexure-based five-bar mechanism for micro/nano manipulation. Sens. Actuators, A **153**, 96–104 (2009)
10. Tian, Y., Shirinzadeh, B., Zhang, D.: Closed-form compliance equations of filleted V-shaped flexure hinges for compliant mechanism design. Precis. Eng. **34**, 408–418 (2010)
11. Gaunekar, A., Göddenhenrich, T., Heiden, C.: Finite element analysis and testing of flexure bearing elements. Cryogenics **36**, 359–364 (1996)
12. Trollier, T., Ravex, A., Crespi, P., Mullié, J., Bruins, P., Benschop, T.: High capacity flexure bearing stirling cryocooler on-board the ISS. Cryocoolers **12**, 31–35 (2003)
13. Deshmukh, S., Gandhi, P.: Optomechanical scanning systems for microstereolithography (MSL): Analysis and experimental verification. J. Mater. Process. Technol. **209**, 1275–1285 (2009)
14. Gandhi, P., Deshmukh, S., Ramtekkar, R., Bhole, K., Baraki, A.: "on-axis" linear focused spot scanning microstereolithography system: Optomechatronic design, analysis and development. J. Adv. Manuf. Systems **12**, 43–68 (2013)
15. Awtar, S., Mariappan, D.: Experimental measurement of the bearing characteristics of straight-line flexure mechanisms. Precis. Eng. **49**, 1–14 (2017)
16. Wan, S., Xu, Q.: Design and analysis of a new compliant XY micropositioning stage based on Roberts mechanism. Mech. Mach. Theory **95**, 125–139 (2016)
17. Chen, W., Chen, S., Qu, J., Chen, W.: A large-range compliant remote center of motion stage with input/output decoupling. Precis. Eng. **51**, 468–480 (2018)
18. Pham, M.T., Teo, T.J., Yeo, S.H.: Synthesis of multiple degrees-of-freedom spatial-motion compliant parallel mechanisms with desired stiffness and dynamics characteristics. Precis. Eng. **47**, 131–139 (2017)
19. Xu, Q.: A novel compliant micropositioning stage with dual ranges and resolutions. Sens. Actuators, A **205**, 6–14 (2014)
20. Linß, S., Gräser, P., Räder, T., Henning, S., Theska, R., Zentner, L.: Influence of geometric scaling on the elasto-kinematic properties of flexure hinges and compliant mechanisms. Mech. Mach. Theory **125**, 220–239 (2018)
21. Zhao, H., Han, D., Zhang, L., Sheng, S.: Design of a stiffness-adjustable compliant linear motion mechanism. Precis. Eng. **48**, 305–314 (2017)
22. Rubbert, L., Bitterli, R., Ferrier, N., Fifanski, S., Vardi, I., Henein, S.: Isotropic springs based on parallel flexure stages. Precis. Eng. **43**, 132–145 (2016)
23. Herpe, X., Walker, R., Dunnigan, M., Kong, X.: On a simplified nonlinear analytical model for the characterisation and design optimisation of a compliant XY micro-motion stage. Robot. Comput. Integr. Manufacturing **49**, 66–76 (2018)
24. Amoedo, S., Thebaud, E., Gschwendtner, M., White, D.: Novel parameter-based flexure bearing design method. Cryogenics **76**, 1–9 (2016)